Theory of metallic glasses. II. Transport and optical properties

Guang-Lin Zhao,* Yi He, and W. Y. Ching
Department of Physics, University of Missouri–Kansas City, Kansas City, Missouri 64110-2499
(Received 6 November 1989; revised manuscript received 26 February 1990)

The electronic transport and optical properties of a-Ni, a-$Mg_{1-x}Zn_x$, and a-$Cu_{1-x}Zr_x$ metallic glasses have been studied based on the first-principles electronic-structure results. The calculation provides a direct test for the theory of quantum coherence for the electronic transport process in disordered metals. The calculated low-temperature resistivity values are in good agreement with experiments for all three glass systems. It is shown that the transport properties of metallic glasses are controlled by the magnitude and the shape of the conductivity function, which appears to have a local minimum near the Fermi energy. For a stable glass, the existence of this local minimum gives rise to a negative temperature coefficient of the resistivity, which is purely due to the elastic disorder scattering of the conduction electrons. The Mooij correlation is explained in terms of the competition between this effect and the positive resistivity contribution from the electron-phonon interaction. The phenomenon of resistivity saturation is explained by a model of equivalence of the configurations of "perfect" amorphous scattering media. The calculated optical conductivity is in reasonable agreement with limited experimental data. The optical-property calculation at low frequency provides a direct computation of the Drude term for optical transitions in metallic systems.

I. INTRODUCTION

The transport properties of metallic glasses (MG's) have been the subject of numerous experimental and theoretical studies for many years.[1] Many interesting and intriguing physical phenomena unique to disordered alloys have been observed and investigated.[2–7] Among them are the negative temperature coefficient (NTC) of resistivity, the Mooij correlation for resistivity and thermopower, resistivity saturation, sign reversal of the Hall coefficient, the observation of superconductivity, negative magnetoresistance, etc. A large number of theoretical models have been suggested to explain and interpret these data. The more well-known ones include the generalized Ziman model[8] and its extension,[9,10] which are essentially based on a free-electron model, the Mott s-d scattering model,[11] the s-d hybridization model,[12,13] the two-level tunneling model,[14–16] phonon-assisted-hopping model[17–19] and, more recently, the weak-localization model based on the idea of quantum interference and coherence.[20–23] Most of these models usually can explain a specific set of data or a specific class of MG, but fail on other instances. The models based on the scattering by free electrons are inherently unsatisfactory, even after substantial efforts of modification. This is because the wave vector $\mathbf{k}$ in a structurally disordered solid has very little physical meaning. One might have argued that in MG, short-range order (SRO) exists as is evidenced by the first peak in the static structure factor $S(\mathbf{q})$. The momentum vector $\mathbf{q}$ can then be related to the $\mathbf{k}$-space concept in developing a free-electron-like theory; the width of the peak in $S(\mathbf{q})$ should contain the information about the SRO of a particular glass. However, such theories contain too many assumptions which are not always satisfied.[7] The microscopic details of the SRO and the effect of the immediate-range order are not accurately built into the theory and many physical parameters such as the electron mean free path, the number of conduction electrons per atom, the density of states (DOS) at the Fermi level (E_F), and the magnitude of Fermi vector are not precisely known for a given system under study. In recent years, there is evidence that the theory based on weak localization is quite successful in explaining many transport properties of MG.[7,21,23,24] Yet this theory is sufficiently general that in applying it to a specific system, one still has to estimate some of the important physical parameters in order to be able to compare with experimental measurements. It is therefore highly desirable that large-scale quantum-mechanical calculations of transport properties on a few selected MG systems be performed to complement the formal theory, and to provide additional insight about the scattering process in such disordered systems at the microscopic level.

In this paper, we present the results of such large-scale calculations on the transport properties on three representative MG systems, namely a-Ni, a-$Mg_{1-x}Zn_x$, and a-$Cu_{1-x}Zr_x$. The electronic properties of these three glasses have been discussed in the preceding paper[25] (referred to thereafter as I) and some preliminary results have been presented.[26] Each of these glass systems has very unique transport properties and a coherent explanation for all of them is a formidable challenge to any of the theoretical models. In spite of the very intensive theoretical effort to understand the electronic processes in disordered solids in recent years, there exists very little direct calculation of the transport properties of MG,[27] especially those involving transition metal elements with tightly bonded d electrons. Others resort to mathematical approximations that are not always justifiable. Most of the theoretical explanations of transport properties on MG

have to be inferred from the calculated DOS spectra, while an accurate determination of DOS is itself still a subject of intense effort by many researchers in this field. In our approach, the calculation of transport properties is based on the direct evaluation of the energy-dependent conductivity function σ_E, using the Kubo-Greenwood formula.[28] Ballentine and co-workers[29] also studied the transport properties of liquid metals using the recursion method and a linear combination of atomic orbitals (LCAO) basis on clusters of a few hundred atoms. Quite satisfactory results were obtained for several single-component liquid metals if the LCAO parameters were carefully chosen. In our approach, the calculation utilizes the electronic-structure results of paper I.[25] There are several advantages to this approach in addition to the fact that our electronic-structure results are state-of-the-art. First, the direct-space approach circumvents entirely the **k**-space concept, which is ill-defined for MG. Second, the direct computation of σ_E avoids many approximations employed in other theories for transport properties. Some of these approximations are not always transparent and the validity of the results is difficult to assess. Third, the first-principles nature of our calculation implies that the effects of quantum coherence, *s-d* hybridization, *d*-band conduction, and localization effect are all implicitly taken into account. The effect of an electron-electron interaction is treated at the level of local density functional theory upon which the calculation of the electronic structures was based. Finally, our approach is not limited to any specific class of MG other than some subtle points involving computational details, which will be clarified whenever needed.

There has not been much experimental work on the optical properties of MG,[30–37] and even less theoretical efforts. It may have been conceived that the optical spectrum of a MG could not be very interesting because it would most likely be featureless, in contrast to the crystalline solids where the Van Hove singularities give rise to structure-rich optical spectra. We find the study of optical transitions in MG to be highly interesting. Precisely because of the absence of the translational symmetry in a structurally disordered solid, the concept of band structure [$E(\mathbf{k})$ dispersion] is no longer valid and there is no distinction between interband and intraband optical transitions. At low photon frequency, the usual Drude term,[38] which is approximated by the formula $\sigma_D = \mathrm{Ne}^2\tau/m^*(1+\omega^2\tau^2)$ (τ is the relaxation time and m^* is the effective mass of the conduction electrons), can be calculated exactly in the case of MG subject only to the size of the structure model. We shall study the results of such a calculation for the three different MG's.

The plan of this paper is outlined as follows. We will first describe the method of transport and optical calculation in Sec. II. The results of transport properties will be presented in Sec. III and those of optical properties in Sec. IV. These results are discussed further in Sec. V with some concluding remarks made in Sec. VI.

II. METHOD

In paper I, we have calculated the energy eigenvalues and eigenfunctions for the three MG's using the OLCAO method and large unit cells with periodic boundary conditions. The wave functions thus obtained can be used to evaluate an energy-dependent conductivity function σ_E according to the Kubo-Greenwood formula:[28]

$$\sigma_E = \frac{2\pi\hbar e^2}{2m^2\Omega} \sum_{\substack{n,m \\ (n\neq m)}} |\langle n|\mathbf{P}|m\rangle|^2 \delta(E_n - E)\delta(E_m - E) \ . \tag{1}$$

The double summation is over all energy states and the double δ function describes the scattering process of an electron at energy E_n to that of energy E_m. $\langle n|\mathbf{p}|m\rangle$ is the momentum matrix element (MME) between states $\langle n|$ and $|m\rangle$. With the OLCAO method, the MME takes the form

$$\begin{aligned}\langle n|\mathbf{p}|m\rangle &= \int \Psi_n^*(\mathbf{k},\mathbf{r})\mathbf{p}\Psi_m(\mathbf{k},\mathbf{r})d^3r \\ &= \sum_{R_\mu} e^{i\mathbf{k}\cdot\mathbf{R}_\mu} \sum_{\substack{i,\alpha, \\ j,\beta}} C_{n,i\alpha}^*(\mathbf{k})C_{m,j\beta}(\mathbf{k}) \int u_i^*(\mathbf{r}-\mathbf{r}_\alpha)\nabla u_j(\mathbf{r}-\mathbf{R}_\mu-\mathbf{r}_\beta)d^3r \ ,\end{aligned} \tag{2}$$

which can be evaluated exactly without resorting to any approximations. In Eq. (2), $C_{n,i\alpha}$ are the eigenvector coefficients of the wave function of the nth band and $u_i(\mathbf{r}-\mathbf{r}_\alpha)$ is the ith atomic orbital centered on the atom α. $\mathbf{R}_\mu$ is the lattice translational vector of the supercell. $u_i(r)$ are themselves expressed as a linear combination of Gaussian-type orbitals (GTO) so that the integrals in (2) can be expressed as a multiple sum of integrals of the gradient operator over GTO.

The temperature-dependent dc conductivity $\sigma(0,T)$ can be obtained from σ_E through

$$\sigma(0,T) = \int \left[-\frac{\partial f(E)}{\partial E} \right] \langle \sigma_E \rangle dE \ , \tag{3}$$

where f is the Fermi distribution function. $\langle \sigma_E \rangle$ implies the configurational average of σ_E. In principle, one should calculate σ_E based on as many independent structural models as possible to obtain the best configurational average. With large models, this is not practical and the configurational average is usually carried out by using the energy eigenvalues and eigenfunctions obtained at several different "k" points of the

quasi-Brillouin-zone.

The temperature dependence of $\sigma(0,T)$ is strictly through the Fermi distribution function f. At low temperature, f is a step function at E_F and the conductivity of the MG is simply σ_{E_F}, while the resistivity ρ is given by $1/\sigma_{E_F}$. The resistivity obtained according to (3) is purely due to the elastic scattering of the conduction electrons from the disordered atoms in the glass. The MME and the distribution of energy E_m contain all the information about the quantum coherence and multiple scattering associated with the electron transport. Expression (3) is valid only at low temperature. As the temperature is increased, the electron-phonon (e-p) interaction, which is totally ignored in the present calculation, may become important.

It should be pointed out that in a calculation with a finite number of atoms in the model, the energy spectrum is discrete instead of continuous as would be the case for a real amorphous solid. This discrete energy spacing implies that the δ-function condition in Eq. (1) can never be satisfied at all energies. This difficulty is circumvented by replacing each discrete energy level by a Gaussian of unit area and a finite width. The larger the model, the smaller the width of the Gaussian should be and the more closely related would be the description for the amorphous system. A similar approach has been used by Ballentine,[29] although he used a cluster model and a quite different computational method. In the present work, the δ function in expression (1) is replaced by a Gaussian function with a width of about 0.03 eV. This corresponds roughly to the separation in energy levels near the Fermi level. The accuracy in determining σ_E, ρ, or σ_{E_F} depends critically on the state density at the Fermi level, which is different for different MG. In a system such as a-Ni, the DOS at E_F is high, and one may obtain reasonably accurate values of ρ with a modest size model. However, for a free-electron-like MG such as a-$Mg_{1-x}Zn_x$, the DOS at E_F is very low, and a calculation based on a larger model to increase the statistics of the energy sampling would be desirable. We shall return to this point when specific results are discussed.

The conductivity function σ_E is the principal part of our calculation of transport properties in MG. From this function, a number of other physical properties can be derived. The thermopower $S(T)$ is given by

$$S(T)=\frac{1}{\sigma(0,T)}\frac{K}{e}\int\langle\sigma_E\rangle\frac{E-E_F}{KT}\frac{\partial f(E)}{\partial E}dE \ . \quad (4)$$

Because $S(T)$ involves the derivatives of the log of the conductivity function, it is even more difficult to evaluate accurately; not only σ_E at E_F, but also its derivatives near E_F must be accurately determined. For that reason, we can at most expect the correct sign and magnitude for $S(T)$ in the present calculation.

It is also possible to define approximately an average electron mobility in a given MG by writing $\langle\sigma_E\rangle$

$$\langle\sigma_E\rangle=\frac{2\pi\hbar e^2}{3m^2\Omega}\overline{|\langle n|\mathbf{P}|m\rangle|^2_E}\sum_{\substack{n,m\\(n\neq m)}}\delta(E-E_n)\delta(E-E_m)$$

$$=\frac{2\pi\hbar e^2}{3m^2\Omega}\overline{|\langle n|\mathbf{P}|m\rangle|^2_E}[N(E)]^2$$

or

$$\langle\sigma_E\rangle=|D_E|^2_{\rm av}[N(E)]^2 \ . \quad (5)$$

The $|D_E|^2_{\rm av}$ defined above gives an approximate measure of the mobility of a single electron at energy E and is somewhat different from that defined in Ref. 1.

The real part of the frequency-dependent optical conductivity $\sigma_1(\omega)$ can be calculated straightforwardly, using the same MME as in the conductivity function calculation:

$$\sigma_1(\omega)=\frac{2\pi e^2h}{3m^2\omega\Omega}\times\sum_{n,l}|\langle n|\mathbf{P}|l\rangle|^2 f_l(1-f_n)\delta(E_n-E_l-\hbar\omega) \ . \quad (6)$$

The MME in (6) is averaged over three Cartesian directions since we expect the optical properties of a MG to be isotropic. The imaginary part of the dielectric function ϵ_2 can be obtained from σ_1

$$\epsilon_2(\omega=4\pi\sigma_1(\omega)/\omega \ , \quad (7)$$

and the real part of the dielectric function can be extracted from ϵ_2 through the usual Kramers-Kronig relation

$$\epsilon_1(\omega)=1+\frac{2}{\pi}\mathrm{P}\int_0^\infty\frac{s\epsilon_2(s)}{s^2-\omega^2}ds \ . \quad (8)$$

The integration limit in (8) has to be replaced by a finite cutoff value, since $\sigma_1(\omega)$ is calculated only for a finite range of photon frequencies. In the present calculation, dipole transitions up to an energy interval of 10 eV are included. The results are then linearly extrapolated to a higher-energy cutoff in the numerical evaluation of (8).

It is sometimes convenient to express ϵ_2 into optical absorption power to have a more direct comparison with experiment. This is carried out through the expression

$$\alpha(\omega)=\epsilon_2(\omega)/\lambda \ . \quad (9)$$

In the electronic-structure calculation of paper I, we used 200-atom models for all three MG systems. Then the same models are used for the transport calculation except for a-Ni, in which the 100-atom model is used. For the optical calculation, the computational resource needed is even more demanding because dipole transitions between each pair of energy levels need to be considered. For that reason, the optical calculations have to be carried out with smaller models containing 100 atoms for a-Ni and 150 atoms for a-$Cu_{60}Zr_{40}$. The same 200-atom model is used for optical calculation in a-$Mg_{70}Zn_{30}$. The smaller model size could affect the accuracy of the result, especially on the transport properties, mainly because of the reduced statistics in the energy eigenstate distribution. For optical results, the only effect of smaller

size model is in the extremely low-frequency range. We will comment further on this point in later sections.

III. RESULTS OF TRANSPORT CALCULATION

A. *a*-Ni

The calculated $\langle \sigma_E \rangle$ averaged over configurations of eight k points for the 100-atom *a*-Ni model[35] is shown in Fig. 1. Also shown is the average mobility $|D_E|^2_{\rm av}$ as defined by Eq. (5). A distinct feature of $\langle \sigma_E \rangle$ is that there exists a minimum in $\langle \sigma_E \rangle$ near E_F. This feature is very important in understanding the physical process of electron transport in MG. The low conductivity value near E_F is consistent with the localized nature of the electron wave functions near and above E_F (see paper I for details). For the same reason the mobility D_E is also quite small for *a*-Ni. The calculated temperature-dependent resistivity $\rho(T)$ and thermopower $S(T)$ are shown in Fig. 2. In the temperature range of 0–200 K, the temperature coefficient of resistivity α is negative in agreement with experimental observation.[39] The calculated thermopower at low temperature is also negative and decreases rather rapidly as temperature is increased. We are not aware of any thermopower data for *a*-Ni to compare with our result. The measured room-temperature resistivity is about 100 $\mu\Omega$ cm, which is close to the calculated value of 111 $\mu\Omega$ cm at 200 K. However, it must be pointed out that *a*-Ni is metastable and very difficult to fabricate. The experimental data on the resistivity of *a*-Ni is scattered and presumably very much sample dependent. The liquid-metal data for Ni,[40] which give a resistivity of 85–87 $\mu\Omega$ cm, may be more reliable.

The calculated transport properties of *a*-Ni are summarized in Table I.

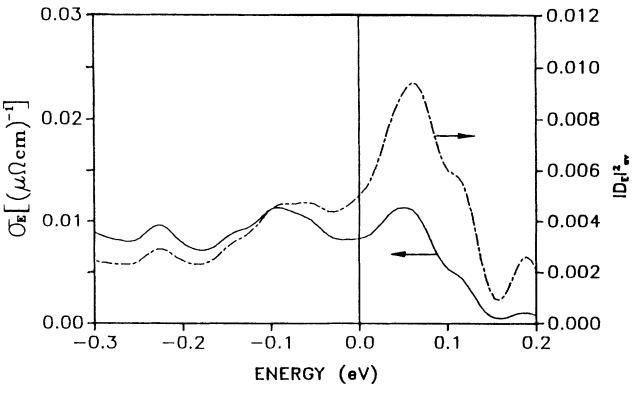

FIG. 1. Conductivity function $\sigma(E)$ (left-hand scale) and average mobility $D(E)$ (right-hand scale) for *a*-Ni calculated with 100-atom model.

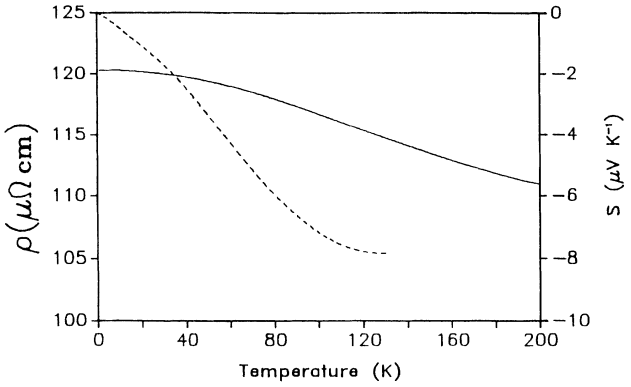

FIG. 2. Resistivity $\rho(T)$ (solid line) and thermopower $S(T)$ (dashed line) for *a*-Ni calculated with 100-atom model.

B. *a*-$Mg_{1-x}Zn_x$

a-$Mg_{1-x}Zn_x$ is a free-electron-like MG with a much smaller resistivity than *a*-Ni. The calculated conductivity functions for $x=0.30$ and 0.25 are shown in Fig. 3. Configurational averages for $\langle \sigma_E \rangle$ are carried out over eight k points of the quasi-Brillouin-zone of the 200-atom model. For both compositions, $\langle \sigma_E \rangle$ again has a local minimum around E_F, which is similar to *a*-Ni. The calculated $\rho(T)$ for both compositions are shown in Fig. 4. It shows that *a*-$Mg_{1-x}Zn_x$ also has a negative α in contrast to the Mooij correlation.[41] This unique experimental observation for *a*-$Mg_{1-x}Zn_x$ glass has not yet been satisfactorily explained by any theoretical model. Models based on free-electron scattering generally predict a positive α for a free-electron-like MG. However, we are unable to explain the experimentally observed fine structures in $\rho(T)$ at low temperature.[42,43]

Our calculated resistivity values for *a*-$Mg_{75}Zn_{30}$ and *a*-$Mg_{75}Zn_{25}$ at $2k$ are 68 and 67.8 $\mu\Omega$ cm, respectively. For coevaporated *a*-MgZn films, a resistivity of 76–85 $\mu\Omega$ cm was reported,[31] while for the melt spinning samples, the resistivity is about 55 ± 5 $\mu\Omega$ cm.[44,45] Our calculated resistivity for *a*-$Mg_{70}Zn_{30}$ lies between these two sets of data as illustrated in Fig. 5.

The thermopower $S(T)$ is more difficult to calculate, especially for *a*-$Mg_{1-x}Zn_x$. Because $S(T)$ is proportional to the derivative of $\langle \sigma_E \rangle$, which is quite small, any numerical inaccuracy, whether it arises from an insufficient configurational average or inadequate cell size, will greatly affect the calculated $S(T)$ values. To obtain an order of magnitude type of estimation, we find it necessary to smooth the $\langle \sigma_E \rangle$ curve in order to obtain $S(T)$ values comparable to that of experiment.[46–48] These are shown in Fig. 6. As mentioned earlier, our calculation shows that there exists a minimum in $\langle \sigma_E \rangle$ around E_F. Because the derivative of $\langle \sigma_E \rangle$ at the two sides of the minimum will have different signs (+ or −), so a small shift of E_F or $\langle \sigma_E \rangle$ can give different signs for the thermopower. Our calculated value for $S(T)$ is -0.95 μVK^{-1} and appears to be in good agreement with one of the published data of -0.80 μVK^{-1}.[47] However, it was pointed out by Muir[49] that the correct experimental value

should be $-0.20\ \mu VK^{-1}$,[48] thus nullifying the good agreement claimed.[26] In any case, we can expect at most the correct order of magnitude for the calculated $S(T)$ value. The calculated and experimental values of $\rho(T)$, $S(T)$, and the temperature coefficients are summarized in Table I.

C. a-$Cu_{1-x}Zr_x$

The transport properties of a-$Cu_{1-x}Zr_x$ MG are well studied experimentally,[45,50–60] This is a nonmagnetic glass with a high resistivity, which means that the conduction electrons undergo strong scattering from the topologically disordered atoms. Clearly, a free-electron-like type of theory will not be applicable and a direct space, first-principles type of calculation is necessary. Our calculated conductivity functions for a-$Cu_{60}Zr_{40}$ and a-$Cu_{50}Zr_{50}$ are shown in Fig. 7. Again, there exists a minimum in $\langle \sigma_E \rangle$ around the Fermi energy similar to a-Ni and a-$Mg_{1-x}Zn_x$. The temperature-dependent resistivity for a-$Cu_{60}Zr_{40}$ and a-$Cu_{50}Zr_{50}$ are shown in

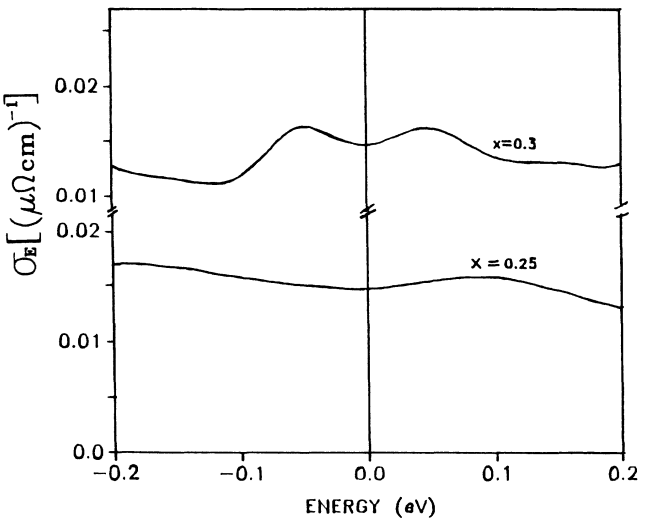

FIG. 3. Conductivity functions near E_F for a-$Mg_{70}Zn_{30}$ and a-$Mg_{75}Zn_{25}$.

TABLE I. Transport properties of a-$Cu_{1-x}Zr_x$, a-$Mg_{1-x}Zn_x$, and a-Ni. The asterisk denotes experiment at 300 K. The dagger denotes experiment at 160 K.

Metallic glass	ρ ($\mu\Omega$ cm) Theory (2 K, 200 K)	S ($\mu V K^{-1}$) Theory (160 K)	$\frac{1}{\rho}\frac{d\rho}{dT}$ (K^{-1}) Theory (200 K)
a-$Cu_{50}Zr_{50}$ (200 atoms)	192.4,185.7	2.04	-2.70×10^{-4}
	177±3[a,b,*]	1.40[e,†]	
	200[c,*]	1.50[f,†]	
	210±20[d*]		
a-$Cu_{60}Zr_{40}$ (200 atoms)	196.6,182.2	2.01	-4.12×10^{-4}
	195[g,*]		
	182.0[h,*]	1.40[e,†]	
	179±3[a,*]		
a-$Mg_{70}Zn_{30}$ (200 atoms)	68.0,65.4	−0.47	-8.5×10^{-5}
	≅56[m,*]		
	76–85[n,*]	−0.58[l,†]	
a-$Mg_{75}Zn_{25}$ (200 atoms)	67.8,67.2	−0.95	-2.0×10^{-5}
	55±5[i,*]	−0.2[p,†]	
	−75[j,*]		
a-Ni (100 atoms)	120.3,110.8	−7.79 (120 K)	3.97×10^{-4}
	~100[k,*]		
	85–87[o,*]		

[a]Reference 55.
[b]Reference 52.
[c]Reference 56.
[d]Reference 57.
[e]Reference 53.
[f]Reference 58.
[g]Reference 50.
[h]Reference 51.
[i]Reference 42.
[j]Reference 43.
[k]Reference 39.
[l]Reference 46.
[m]Reference 44.
[n]References 30 and 31.
[o]Reference 40.
[p]Reference 47.

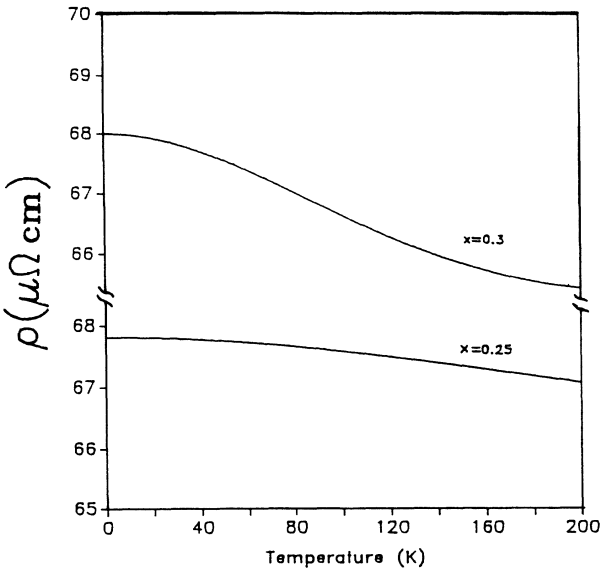

FIG. 4. Calculated $\rho(T)$ for a-$Mg_{70}Zn_{30}$ and a-$Mg_{75}Zn_{25}$.

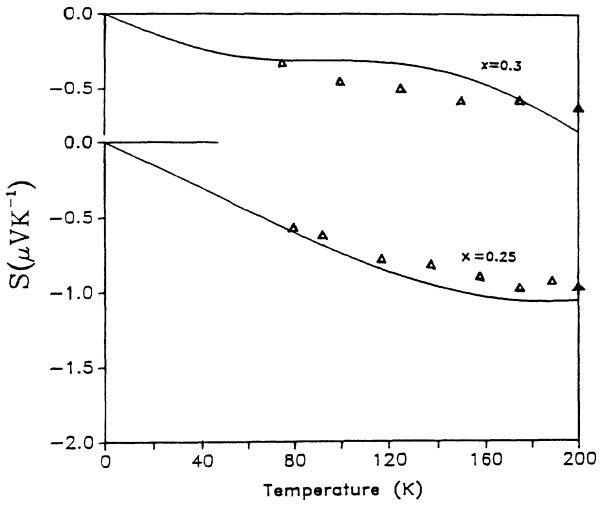

FIG. 6. Comparison of calculated and experimental values of $S(T)$ for a-$Mg_{70}Zn_{30}$ and a-$Mg_{75}Zn_{25}$.

Fig. 8. The reduced resistivity $\rho(T)/\rho(2k)$ and the experimental data are shown in Fig. 9. For both compositions, a negative α is obtained in agreement with experiment.[51] At low temperature, the calculated resistivity is in close agreement with the measured data,[50] especially for a-$Cu_{60}Zr_{40}$. At a higher temperature ($T > 150$ K), the calculated resistivity starts to deviate from the measured one with a faster decrease in ρ as T is increased. It should be reminded that our calculation does not include the contribution to $\rho(T)$ due to the e-p interaction. Apparently, as the temperature is increased, the e-p interaction starts to set in, which gives a positive contribution to $\rho(T)$. The calculated resistivity values at low temperature for both a-$Cu_{60}Zr_{40}$ and a-$Cu_{50}Zr_{50}$ are 197 and 192 $\mu\Omega$ cm, respectively. The experimental values range from 180 to 250 $\mu\Omega$ cm.[50-60] Considering the uncertainty in the measurements under different experimental conditions, we consider the agreement to be quite satisfactory. The calculated thermopower $S(T)$ for a-$Cu_{60}Zr_{40}$ and a-$Cu_{50}Zr_{50}$ are shown in Fig. 10 together with some experimental data.[60] The agreement is not as good as in a-$Mg_{1-x}Zn_x$ glasses, but the calculation still gives the correct sign for $S(T)$. Again it must be reminded that

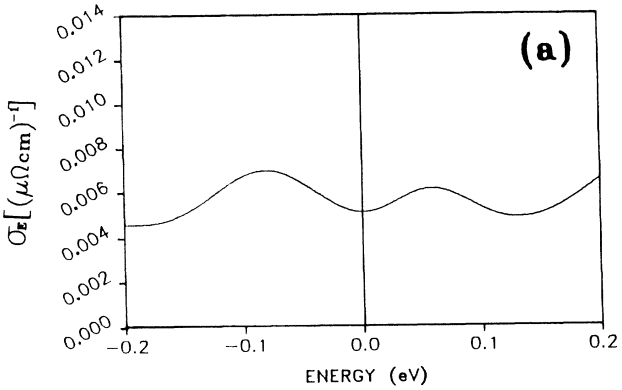

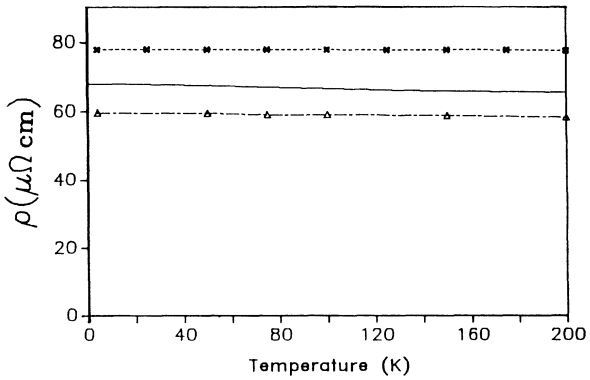

FIG. 5. Comparison of calculated $\rho(T)$ (solid line) of a-$Mg_{70}Zn_{30}$ with experiments. Dashed line, data from Refs. 30 and 31; dash-dotted line, data from Ref. 44.

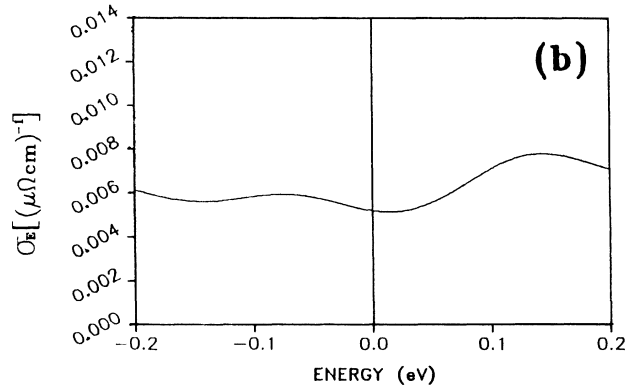

FIG. 7. Calculated conductivity function σ_E near E_F for a-$Cu_{1-x}Zr_x$. (a) a-$Cu_{60}Zr_{40}$; (b) a-$Cu_{50}Zr_{50}$.

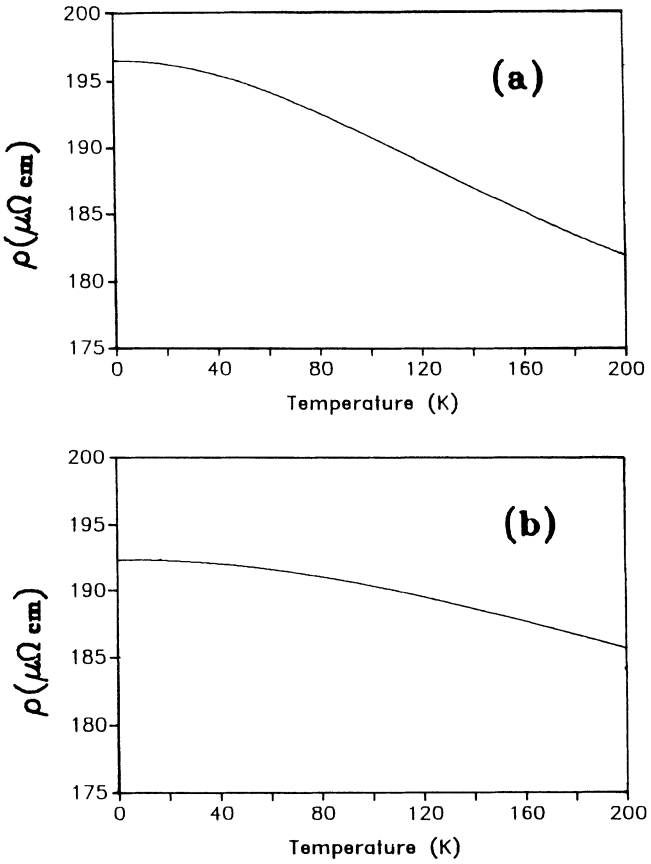

FIG. 8. Calculated $\rho(T)$ for (a) a-$Cu_{60}Zr_{40}$ and (b) a-$Cu_{50}Zr_{50}$.

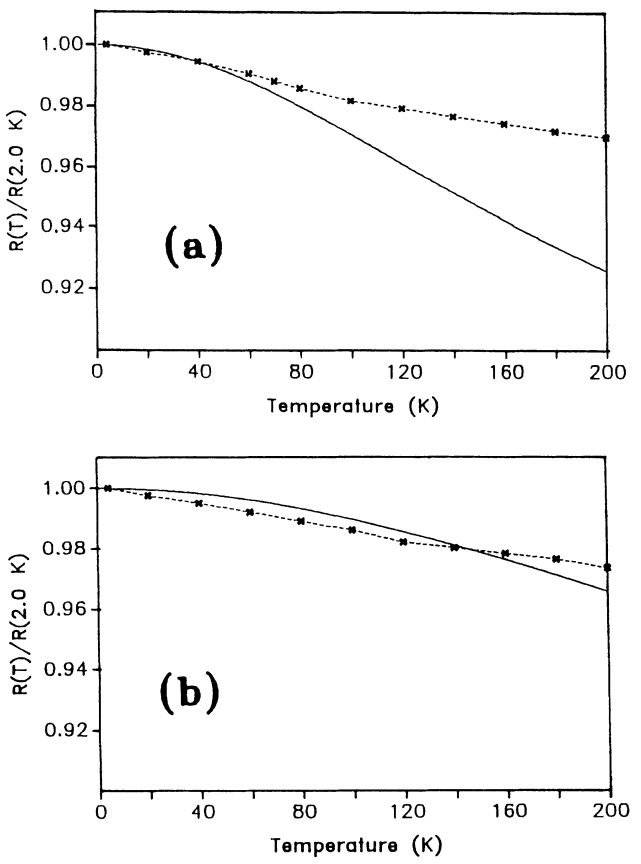

FIG. 9. Comparison of calculated $\rho(T)$ (solid line) with experiment (dashed line from Ref. 48) for (a) a-$Cu_{60}Zr_{40}$ and (b) a-$Cu_{50}Zr_{50}$.

calculation for the thermopower at a higher temperature is not expected to be accurate since the e-p interactions are neglected.

We also have used the case of a-$Cu_{60}Zr_{40}$ to test the sensitivity of our result on the models of different sizes. We obtained the conductivity values at the Fermi level $\sigma_E(E_F)$ to be 0.0057, 0.0055, and 0.0052 $(\mu\Omega\,\mathrm{cm})^{-1}$ for the 100-, 150-, and 200-atom models, respectively. The calculation on the 100-atom model is averaged over eight **k** points as in the case of a-Ni. This test shows a reasonably stable result with regard to the model size. However, no extensive tests on many differently prepared models have been attempted and we are unable to test models with size larger than 200 atoms. The calculated transport properties for the a-$Cu_{1-x}Zr_x$ glass, together with experimental data, are summarized in Table I.

IV. RESULTS ON OPTICAL CALCULATIONS

A. a-Ni

For the optical calculations, the amount of computational time required increases dramatically even for a modest photon-energy range of about 10 eV. This is because each pair of transitions from a state below E_F to a state above E_F needs to be considered. For that reason the calculation of optical properties of a-Ni according to Eq. (6) has to be limited to the 100-atom model. The calculated real part of optical conductivity $\sigma_1(\omega)$ for a-Ni is shown in Fig. 11(a). It is clear that below 0.5 eV, the optical absorption increases dramatically, which is characteristic of a Drude type of behavior. There appear to be some broad structures at 1.0, 2.5, 4.0, and 5.2 eV which need detailed experimental data to confirm. In the same diagram, we have plotted the experimental data on optical conductivity from c-Ni (Ref. 61) for comparison. Our calculation gives the right order of magnitude for $\sigma_1(\omega)$. Most important is that the Drude type of absorption at low photon energy is well reproduced. In Fig. 11(b), the converted real and imaginary parts of the dielectric function are presented. Also shown are the recent optical data on a-$Ni_{95}Tb_{0.5}$.[29] The agreement is reasonably satisfactory.

b. a-$Mg_{70}Zn_{30}$

The optical properties of a-$Mg_{70}Zn_{30}$ have been calculated based on the 200-atom unit cell. The calculation is limited to transition energies of less than 10 eV. The results are shown in Fig. 12. At low energy, a Drude type of absorption is even more evident since a-$Mg_{70}Zn_{30}$ is expected to be free-electron-like. Also shown in Fig. 12(a) is the experimental data of Theye *et al.*[43] Above 2 eV, the agreement with experiment is excellent. Both the calculation and the data show a featureless, graduate de-

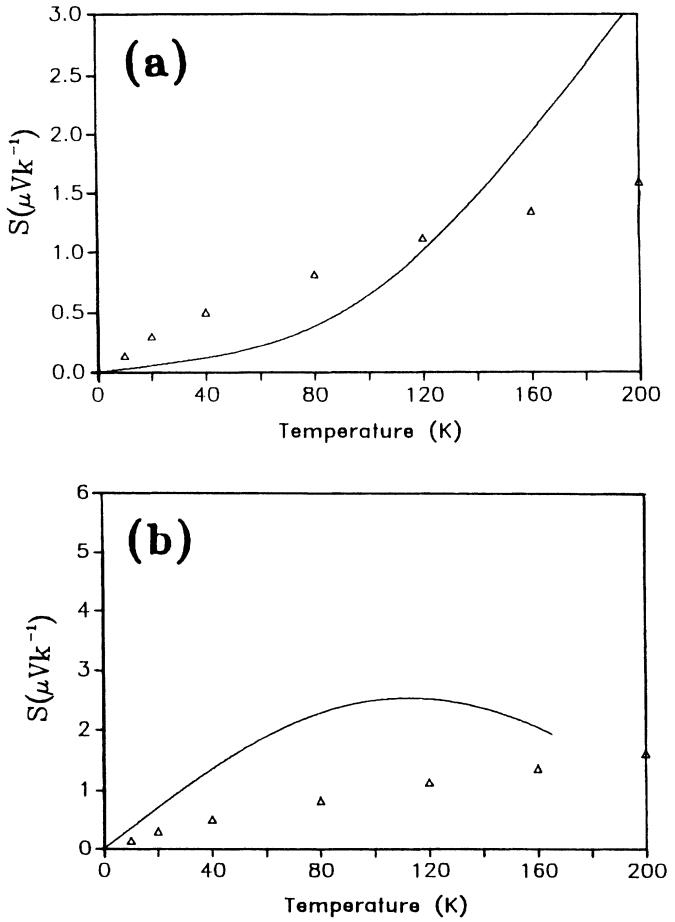

FIG. 10. Comparison of calculated (solid line) and experimental values (Δ) from Refs. 48 and 57 of $S(T)$ for (a) a-$Cu_{60}Zr_{40}$ and (b) a-$Cu_{50}Zr_{50}$. $Cu_{50}Zr_{50}$.

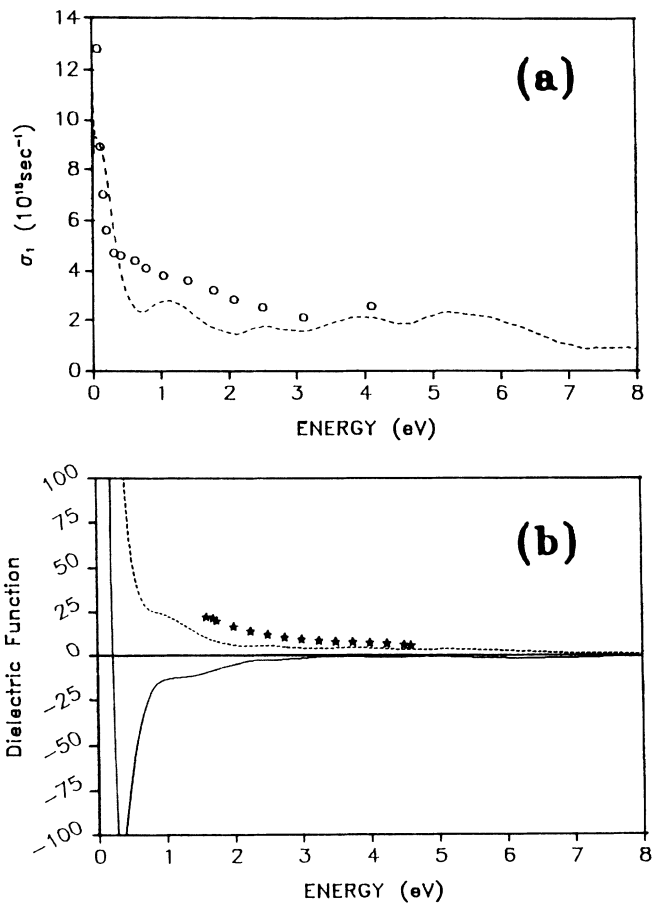

FIG. 11. Calculated optical properties of a-Ni: (a) $\sigma_1(\omega)$; ○ represent experimental data for c-Ni from Ref. 60. (b) Calculated dielectric function for a-Ni. * represent the experimental data from Ref. 29.

creasing absorption. This result is consistent with a rather featureless DOS above and below E_F for a-$Mg_{70}Zn_{30}$ (see paper I, Fig. 6). Below 2 eV, the calculation predicts a stronger absorption than the data had indicated. This kind of discrepancy is quite common for optical absorption calculations. Clearly, more experimental measurements are called for.

In Figs. 11(b) and 11(c), the converted data for the dielectric function and the reflectivity for a-$Mg_{70}Zn_{30}$ are illustrated. At low energy, the dielectric function of a-$Mg_{70}Zn_{30}$ is much higher than that of a-Ni. This again shows that the conduction electrons in a-$Mg_{70}Zn_{30}$ are much more free-electron-like. The reflectivity of a-$Mg_{70}Zn_{30}$ decreases monotonically with photon energy and is smaller than 0.03 above 7 eV.

C. a-$Cu_{50}Zr_{50}$

Because of limitations on computer resources, the calculation of optical properties of an a-$Cu_{1-x}Zr_x$ alloy is limited to one composition, a-$Cu_{50}Zr_{50}$, and that of a 150-atom model. The 150-atom model is constructed in the same manner as the 200-atom model and gives the same radial distribution function and electron DOS spectra. The calculated real part of optical conductivity, the dielectric function, and the absorption power are shown in Fig. 13. At low energy (below 0.3 eV), a similar Drude type of behavior is again quite evident. The main features are the existence of some minima in the background of a gradually decreasing absorption up to 8 eV. These minima are located at photon energies of 0.3, 0.7, and 3.4 eV. We find only one preliminary experimental datum[32] for comparison. This is shown in Fig. 13(c) for the absorption spectrum. The agreement is reasonably satisfactory, although the calculation seems to overestimate the strength of absorption. But again, this type of disagreement is quite common, especially for systems that are very much sample dependent.

V. DISCUSSION

From the above results of the transport properties of three very different MG's, it is obvious that such first-principles calculations include all the effects of multiple scattering, localization, and quantum interference effects within the limitations of the local density theory and the underlining structural model. This is because all the

SRO's and intermediate-range orders are included in the calculation. The elastic electronic scattering in the disordered medium, irrespective of the strength of the scatterers, is treated exactly while the electron-phonon interaction is totally neglected. Such calculations are consistent with the notion of the quantum interference model (or weak localization model) and the results thus obtained can be used to assess the validity of the model. It is gratifying to see that the calculated low-temperature resistivities of all the three MG's are within the experimental uncertainty of the measured values. From the temperature-dependent resistivity, which includes only the effects of elastic disordered scattering, it is clear that all three MG's have negative temperature coefficients α. As the temperature is increased, the e-p interaction becomes increasingly important. If the e-p interaction is not strong enough to overcome the effect of elastic disorder scattering, as is in the case of a-$Cu_{60}Zr_{40}$ of Fig. 13, the temperature coefficient remains negative. For some other MG systems where the elastic disordered scattering is weak, the e-p interaction may be strong enough to overtake the former and gives rise to a positive temperature coefficient.

The above argument leads to a natural explanation for the Mooij correlation,[41] which states that, in general, low resistivity alloys have a positive temperature coefficient and high resistivity alloys have a NTC with crossover

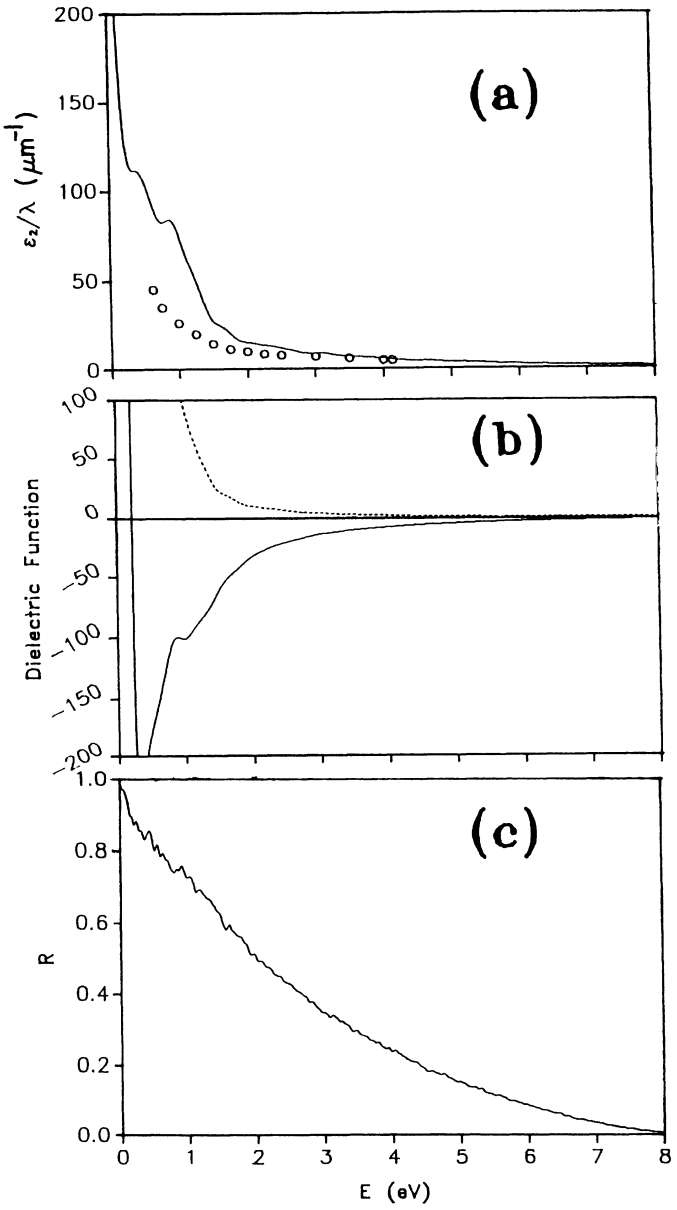

FIG. 12. Calculated optical properties for a-$Mg_{70}Zn_{30}$ using 200-atom model. (a) Absorption spectrum; ○ represent experimental data from Ref. 43; (b) calculated dielectric function for a-$Mg_{70}Zn_{30}$.

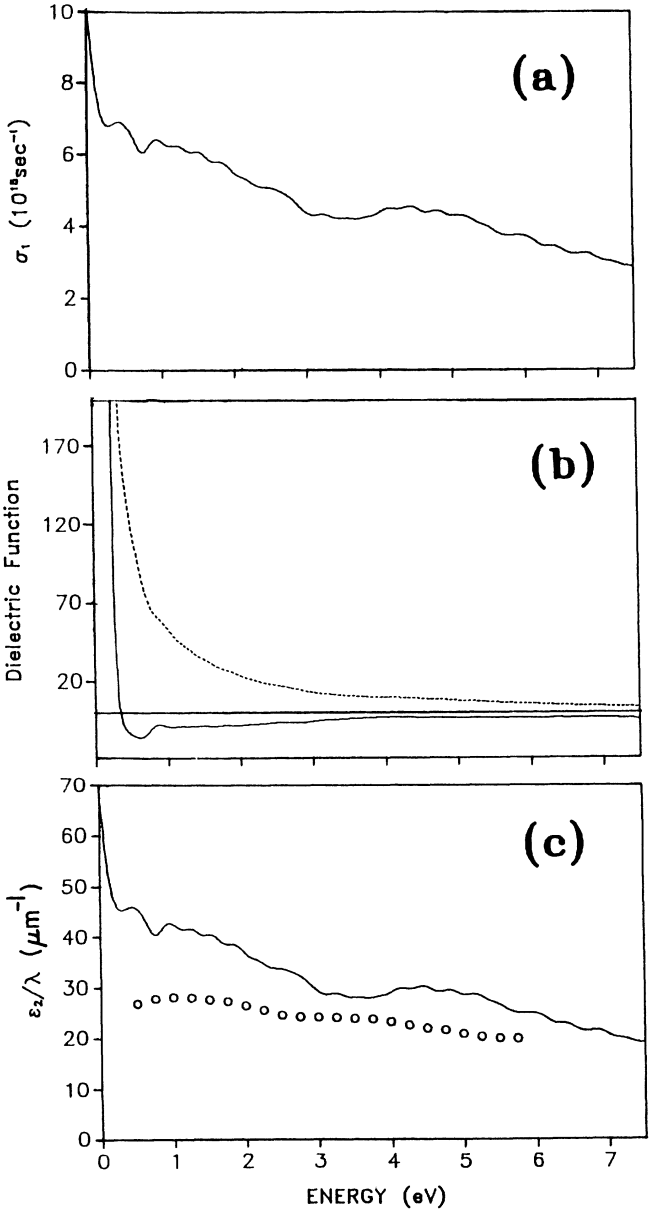

FIG. 13. Calculated optical properties for a-$Cu_{50}Zr_{50}$ using 150-atom model. (a) Optical conductivity; (b) dielectric function; (c) comparison of absorption power with experiment for a-$Cu_{50}Zr_{50}$. ○ represent the experimental data from Ref. 32.

occurring at a resistivity value of about 150 $\mu\Omega$ cm. Let us write the total resistivity $\rho_{\text{tot}}(T)$ as

$$\rho_{\text{tot}}(T)=\rho_{\text{el}}(T)+\rho_{e\text{-ph}}(T)\ , \tag{10}$$

so

$$\alpha_{\text{tot}}=\frac{1}{\rho_{\text{tot}}}\frac{d\rho_{\text{tot}}}{dT}=\frac{1}{d\rho_{\text{tot}}}\frac{d\rho_{\text{el}}}{dT}+\frac{1}{\rho_{\text{tot}}}\frac{d\rho_{e\text{-ph}}}{dT}$$
$$=\alpha_{\text{el}}+\alpha_{e\text{-ph}}\ . \tag{11}$$

Here el and e-ph mean elastic and e-p interaction, respectively. For very good amorphous systems at low temperature, e-p scattering can be ignored so $\rho_{\text{tot}}(T)\cong\rho_{\text{el}}(T)$ and $\alpha_{\text{tot}}\cong\alpha_{\text{el}}$, where ρ_{el} dominates and α_{el} is negative. At finite temperature in a real system, the vibration of atoms will introduce some additional disorder. The e-p interaction cannot be totally ignored and will contribute a positive $\alpha_{e\text{-ph}}$. Therefore it is the competition between the negative α_{el} and the positive $\alpha_{e\text{-ph}}$ that determines the overall sign of α_{tot}. Naturally, the Mooij correlation could not be strictly universal, as pointed out by Tsuei,[62] because the nature of the disorder scattering and the e-p interaction depends on the details of the electronic structure of the system in a much more complicated and subtle way than simply suggested by the resistivity values.

Numerous experimental measurements show that almost all disordered metallic alloys tend to have a saturation in resistivity ρ_c at high temperature, independent of the residual resistivity ρ_0 at low temperature.[1,41] A traditional theory of electron-phonon scattering would predict a linear temperature dependence of ρ at high T. This phenomenon of resistivity saturation can be understood based on a model of equivalence of the configurations of "perfect" amorphous scattering medium. We define a perfect amorphous scattering medium to be one whose atoms are randomly distributed according to the short-range interatomic forces and cannot be further disordered. The different atomic configurations of the perfect amorphous system (e.g., at different temperature) are equivalent as far as the scattering effect to the conduction electrons is concerned. This means that the e-p scattering cannot have a significant effect in the perfect amorphous system. At a temperature much higher than, say, the Debye temperature θ_D, the vibrations of atoms will make the real system almost equivalent to a perfect amorphous one, because if the temperature is raised, the system cannot be further disordered. In this case, we shall have $\rho(T_1)\sim\rho(T_2)\sim\rho_c$, where $T_2>T_1\gg\theta_D$. ρ_c is the resistivity that the system becomes equivalent to a perfect amorphous medium. Also ρ_c will be close to the residual resistivity ρ_0 if the system is close to an ideal amorphous solid which is almost equivalent to a perfect one at low T.

The most fundamental quantity that controls the transport properties of MG is its conductivity function $\langle\sigma_E\rangle$. Of particular importance is the functional behavior of $\langle\sigma_E\rangle$ near E_F. For all the MG studied in this paper, we find that there exists a minimum in $\langle\sigma_E\rangle$ at or near E_F. We may argue that this is a general property for MG, which has a NTC α and a small thermopower. To see this more clearly, let us expand $\langle\sigma_E\rangle$ in a Taylor series about its minimum at E_F up to, say, fourth order,

$$\langle\sigma_E\rangle=\langle\sigma_0\rangle+\left[\frac{\partial\langle\sigma_E\rangle}{\partial E}\right]_0E+\frac{1}{2!}\left[\frac{\partial^2\langle\sigma_E\rangle}{\partial E^2}\right]_0E^2$$
$$+\frac{1}{3!}\left[\frac{\partial^3\langle\sigma_E\rangle}{\partial E^3}\right]_0E^3$$
$$+\frac{1}{4!}\left[\frac{\partial^4\langle\sigma_E\rangle}{\partial E^4}\right]_0E^4+\cdots\ . \tag{12}$$

We can use the experimentally determined values of $[T,\rho(T)]$ and $[T,S(T)]$ to determine the derivatives of $\langle\sigma_E\rangle$ and hence determine the $\langle\sigma_E\rangle$ curve near E_F. Such experimentally converted $\langle\sigma_E\rangle$ curves are shown in Fig. 14 for a-$Mg_{70}Zn_{30}$ and a-$Cu_{50}Zr_{50}$. These curves are very similar to the ones directly obtained from the first-principles calculations. It can be roughly estimated that for a MG system with $[\rho(200K)-\rho(2K)]/\rho(2K)<-0.02$ to -0.01, and $|S(200K)|<5$ to 10 μVK^{-1}, the system is likely to have a minimum in $\langle\sigma_E\rangle$ around E_F.

Many MG systems exhibit resistivity anomalies, which is quite difficult to explain by any theory. They may be related to the detailed structures of $\langle\sigma_E\rangle$ near E_F. Similarly, the thermopower $S(T)$, which is difficult to calculate accurately, is related to the curvatures of $\langle\sigma_E\rangle$. For a system with a minimum in $\langle\sigma_E\rangle$ around E_F and a symmetric curvature on both sides of the minimum, $S(T)$ is likely to be small. It is difficult to calculate $\langle\sigma_E\rangle$ to such a high degree of accuracy. This is probably the reason why our calculated $S(T)$ values listed in Table I generally overestimate the experimentally determined values.

The existence of a minimum in the $\langle\sigma_E\rangle$ curve for all the three MG's can also be related to the relative stability of the glass. Since $\langle\sigma_E\rangle$ is proportional to the transition probability between different states when the system undergoes a disturbance as a result of scattering, a minimum in $\langle\sigma_E\rangle$ at E_F implies that the system is stable against the configurational change. In a given series of

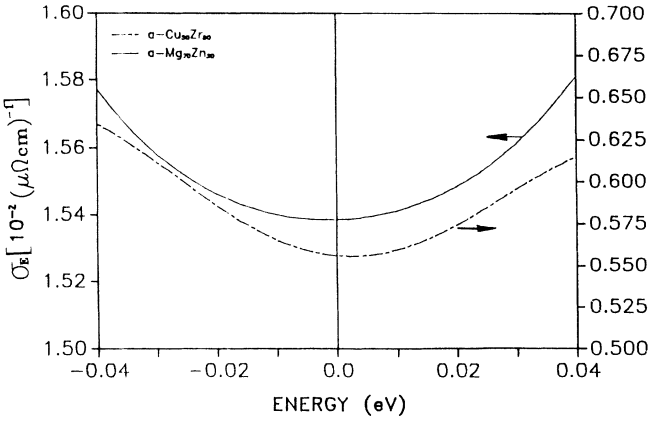

FIG. 14. Converted $\langle\sigma_E\rangle$ curves from experimental data using Eqs. (1), (4), and (12) for a-$Cu_{50}Zr_{50}$ (dash-dotted line) and a-$Mg_{70}Zn_{30}$ (solid line). See text for detail.

binary MG, a composition which gives a deeper minimum in $\langle \sigma_E \rangle$ would indicate a more stable composition. In the a-Cu_xZr_{1-x} series, experimental data indicate that a-$Cu_{60}Zr_{40}$ has a higher resistivity (low σ_E) while being the easiest to form.[45,52] Alternatively, this can be interpreted as indicating that the electronic states at the Fermi level are more strongly affected by the disorder than those immediately above or below the Fermi level. In principle, the stability of a MG should be determined by the total energy of the system in both the electronic and the nuclear coordinate space. While an accurate total energy calculation within the local density approximation becomes quite routine for simple crystals, such a calculation for MG is obviously not possible at the present moment. We speculate that the equilibrium configuration which has a minimum in $\langle \sigma_E \rangle$ at E_F is also the one with a minimum in the total energy. Our conjecture that a stable MG should have a minimum in $\langle \sigma_E \rangle$ at E_F is in contrast to the conclusion based on the free-electron theory which predicts that a stable glass should have a minimum in the DOS curve.[63] However, because of the finite size of the model and the limited statistics for states near the Fermi level, we must caution the readers that our interpretation of a minimum at E_F in $\sigma(E)$ is admittedly speculative even though such minima were obtained for all three metallic glass systems studied.

The results of the optical properties calculation show good agreement between the theory and experiments. Of particular significance is the result of optical transition at low frequency, i.e., the Drude term, can be evaluated from first-principles. This is because in amorphous systems, one need not differentiate between the interband and intraband transitions. The information on the scattering process in a disordered environment and the accompanying relaxation process of the conduction electrons are all contained in the electron wave functions, which are calculated from first-principles. It is therefore not necessary to include the lifetime broadening in the optical conductivity calculation of an amorphous system. For crystalline materials, it is often necessary to include a finite lifetime broadening in the calculation in order to have a more direct comparison with the experiment.

VI. CONCLUDING REMARKS

By means of the realistic direct-space calculation on the transport properties of three very different MG's, we have obtained a microscopic understanding of the electronic process in disordered metals. The good agreement between the calculated resistivity values and the experimental data indicates that the local density theory is capable of explaining all major features of transport properties. It is shown that the transport properties of MG are controlled by the conductivity function $\langle \sigma_E \rangle$. The existence of a minimum in $\langle \sigma_E \rangle$ near E_F as a result of elastic disorder scattering gives rise to a NTC α. This minimum in $\langle \sigma_E \rangle$ may also be related to the relative stability of the glass. The Mooij correlation can be explained simply in terms of mutual competition between elastic disorder scattering, which gives a NTC, and that of the electron-phonon interaction, which gives a positive contribution to the temperature coefficient.

The optical conductivity calculation for the same three MG's also gives results in reasonable agreement with a limited number of available experiments. At low frequency, our calculation gives a direct account for the Drude term for the metallic systems.

The present results represent a very realistic calculation for transport properties in MG. Still, further improvements can be made. First, one can always use larger models containing, say, 250–500 atoms per unit cell. This could reduce the numerical noise and lead to higher accuracy, especially in the case of a thermopower calculation.[49] The optical calculation can also be pressed towards an even lower photon frequency. Since the computational time generally increases as N^3, where N is the total number of orbitals involved in a given model of MG, a more practical approach is to carry out the configurational average over calculations with several independent models of modest size. This will increase the required statistics for the number of states involved in the transition process and give a more accurate conductivity function. Second, the accuracy of the wave functions may be improved by an improved electronic-structure calculation as discussed at the end of paper I. Third, for MG containing magnetic atoms, such as Ni or Fe, a spin-polarized calculation may be feasible.[64]

Using the approach and procedure outlined in this paper, we can extend our calculation to other MG systems. For a given compositional series, a first-principles study of the dependence of transport properties on the compositional ratio will be very revealing. For example, the nature of metal-insulator transition[65,66] in a-$Si_{1-x}Cr_x$ or a-$Si_{1-x}Ni_x$ series can be investigated fully. One can also study the temperature dependence or pressure dependence of the transport properties by performing calculations on MG models whose atomic positions are consistent with a given set of temperature and pressure conditions. It is also within reach to study the e-p interaction in MG since such a calculation in crystalline solid has been quite well developed,[67,68] and the present calculation is tantamount to that of a very complicated crystal of null symmetry. These and other studies on MG will be the subjects of future publications.

ACKNOWLEDGMENTS

This work is supported by the U.S. Department of Energy Grant No. DE-FG02-84ER45170.

*Present address: Ames Laboratory–U.S. Department of Energy and Department of Physics, Iowa State University, Ames, Iowa 50011-3020.

[1]N. F. Mott and E. A. Davis, *Electronic Process in Non-crystalline Materials* (Clarendon, Oxford, 1979).

[2]See, for example, *Glassy Metals I and II*, edited by H.-J. Güntherodt and H. Beck (Springer-Verlag, New York, 1981 and 1983).

[3]S. R. Naugel, Adv. Chem. Phys. **51**, 227 (1982).

[4]U. Mizutani, Prog. Mater. Sci. **28**, 97 (1983).

[5]D. G. Nagle, J. Phys. Chem. Solids **45**, 367 (1984).
[6]J. S. Dugdale, Contemp. Phys. **28**, 547 (1987).
[7]M. A. Howson and B. L. Gallagher, Phys. Rep. **170**, 265 (1988).
[8]M. Ziman, Philos. Mag. **6**, 1031 (1961).
[9]T. E. Faber and J. M. Ziman, Philos. Mag. **11**, 153 (1965).
[10]R. Evans, D. A. Greenwood, and P. Lloyd, Phys. Lett. **35A**, 57 (1971).
[11]N. F. Mott, Philos. Mag. **26**, 1249 (1972).
[12]G. F. Weir, M. A. Howson, B. L. Gallagher, and G. J. Morgan, Philos. Mag. **47**, 163 (1983).
[13]G. J. Morgan and G. F. Weir, Philos. Mag. **47**, 177 (1983).
[14]P. W. Anderson, B. I. Halperin, and C. M. Varma, Philos. Mag. **25**, 1 (1972).
[15]R. Cochrane, R. Harris, J. Ström-Olsen, and M. Zuckerman, Phys. Rev. Lett. **35**, 676 (1975).
[16]C. C. Tsuei, Solid State Commun. **27**, 691 (1978).
[17]S. M. Girvin and M. Jonson, Phys. Rev. B **22**, 3583 (1980).
[18]Y. Imry, Phys. Rev. Lett. **44**, 469 (1980).
[19]D. Belitz and W. Götze, J. Phys. C **15**, 981 (1982).
[20]E. Abrahams, P. W. Anderson, D. C. Licciardello, and T. V. Ramakrishnan, Phys. Rev. Lett. **47**, 1617 (1981).
[21]P. A. Lee and T. V. Ramakrishnan, Rev. Mod. Phys. **57**, 287 (1985).
[22]B. L. Alt'shuler and A. G. Aronov, in *Electron-Electron International in Disordered Conductors,* edited by A. L. Efros and M. Pollak (North-Holland, Amsterdam, 1985), p. 4.
[23]M. A. Howson, J. Phys. F **14**, L25 (1984).
[24]M. A. Howson, J. Phys. F **16**, 984 (1986).
[25]W. Y. Ching, G.-L. Zhao, and Y. He, preceding paper, Phys. Rev. B **42**, 10 878 (1990).
[26]G. L. Zhao and W. Y. Ching, Phys. Rev. Lett. **62**, 2511 (1989).
[27]For a detailed review, see Ref. 7.
[28]R. Kubo, Can. J. Phys. **34**, 1274 (1956); D. Greenwood, Proc. Phys. Soc. London **71**, 585 (1958).
[29]L. E. Ballentine, in *Rapidly Quenched Metals,* edited by S. Steeb and H. Warlimont (Elsevier, New York, 1985), p. 981; L. E. Ballentine and J. E. Hammerberg, Can. J. Phys. **64**, 692 (1984).
[30]B. Y . Yang, P. Klosowski, K. Vedam, and J. S. Lannin, Phys. Rev. B **38**, 1562 (1988).
[31]V. Nguyen-Van, S. Fisson and M. L. Theye, J. Non-Cryst. Solids **61&62**, 1325 (1984).
[32]J. Rioory and J. M. Frigerio, *Proceedings of the Fourth International Conference on Rapidly Quenched Metals, Sendal, 1981,* edited by T. Masumoto and K. Suzuki (The Japan Institute of Metals, Sendai, 1981), p. 1287.
[33]H.-J. Güntherodt *et al.*, J. Phys. (Paris) Colloq. **41**, C8-381 (1980).
[34]E. Hauser, R. J. Zirke, J. Tauc, J. J. Hauser, and S. R. Nagel, Phys. Rev. B **19**, 6331 (1979).
[35]S. Ray and J. Tauc, Solid State Commun. **34**, 769 (1980).
[36]A. Schlegel, P. Wachter, K. P. Acfermann, M. Liard, and H.-J. Güntherodt, Solid State Commun. **31**, 373 (1979).
[37]S. W. McKnight and A. K. Ibrahim, Phys. Rev. B **29**, 6570 (1984).
[38]P. Drude, *The Theory of Optics* (Longmans Green, New York, 1902).
[39]As presented in T. Fujiwara, J. Phys. F **9**, 2011 (1979).
[40]T. Iida and R. I. L. Guthrie, in *The Physical Properties of Liquid Metals* (Clarendon, Oxford, 1988), p. 232–233.
[41]J. H. Mooij, Phys. Status Solidi A **17**, 521 (1973).
[42]E. Luescher *et al.*, J. Non-Cryst. Solids **61&62**, 1109 (1984); J. K. Vassilou, J. Appl. Phys. **59**, 492 (1986).
[43]M. L. Theye, Van Nguyen-Van, and S. Fisson, Phys. Rev. B **31**, 6447 (1985).
[44]J. Hafner, E. Gratz, and H. J. Güntherodt, J. Phys. (Paris) Colloq. **41**, C8-512 (1980).
[45]Y. Calvayrac, *et al.*, Philos. Mag. B **48**, 323 (1983).
[46]T. Matsuda and U. Mizutani, J. Phys. F **12**, 1877 (1982).
[47]T. Matsuda, U. Mizutani, W. B. Muir, and M. From, J. Phys. F **14**, L21 (1984).
[48]M. N. Baibich, W. B. Muir, Z. Altounian, and Tu Guo-Hua, Phys. Rev. B **26**, 2963 (1982).
[49]W. B. Muir, Phys. Rev. Lett. **64**, 1180 (1990); W. Y. Ching, *ibid.* **64**, 1181 (1990).
[50]T. Murata, S. Tomizawa, T. Fukase, and T. Masumoto, Scr. Metall. **10**, 181 (1976).
[51]E. Babic, R. Ristic, M. Miljak, and M. G. Scott, in *Proceedings of the Fourth International Conference on Rapidly Quenched Metals, Sendai, 1981,* edited by T. Masumoto and K. Suzuki (The Japan Institute of Metals, Sendai, 1981), Vol. 2, p. 1079.
[52]B. L. Gallagher and D. Greig, J. Phys. F **12**, 1721 (1982).
[53]M. N. Baibich, W. B. Muir, Z. Altounian, and Tu Guo-Hua, Phys. Rev. B **27**, 619 (1983).
[54]G. Fritsch, E. Lüscher, A. Schult, A. Eckert, J. Willer, and W. Dyckhoff, J. Non-Cryst. Solids **61-62**, 1225 (1984).
[55]Z. Altounian and J. O. Strom-Olsen, Phys. Rev. B **27**, 4149 (1983).
[56]O. Rapp, J. Jäckel, and K. Frobose, J. Phys. F **11**, 2359 (1981).
[57]S. Basak, S. R. Nagel, and B. C. Glessen, Phys. B **21**, 4049 (1981).
[58]B. L. Gallagher and B. J. Hickey, J. Phys. F **15**, 911 (1985).
[59]K. Samner and H. v. Löhneysen, Phys. Rev. B **26**, 107 (1982).
[60]H. J. Eifert, B. Elschner, and K. H. Buschow, Phys. Rev. B **25**, 7441 (1982).
[61]M. M. Kirillova, Zh. Eksp. Teor. Fiz. **61**, 336 (1971) [Sov. Phys.—JETP **34**, 178 (1972)].
[62]C. C. Tsuei, Phys. Rev. Lett. **57**, 1943 (1986).
[63]S. R. Nagel and J. Tauc, Phys. Rev. Lett. **35**, 380 (1975).
[64]W. Y. Ching, Y.-N. Xu, B. N. Harmon, J. Ye, and T. C. Leung, Phys. Rev. B **42**, 4460 (1990).
[65]G. Hartel, D. J. Bishop, E. G. Spemer, J. M. Rowell, and R. C. Dynes, Phys. Rev. Lett. **50**, 743 (1983).
[66]S. Okuma, S. Shiratake, A. Asamitsu, and N. Nishida, Solid State Commun. **70**, 1091 (1989).
[67]C. M. Varma and W. Weber, Phys. Rev. Lett. **39**, 1094 (1977); Phys. Rev. B **19**, 6142 (1979).
[68]X. W. Wang, B. N. Harmon, Y. Chen, K. M. Ho, C. Stassis, and W. Weber, Phys. Rev. B **33**, 3851 (1986).